Aerospace Science and Technology 130 (2022) 107877

Contents lists available at ScienceDirect

Aerospace Science and Technology

www.elsevier.com/locate/aescte

Controller design and stability analysis for spinning missiles via tensor product

Zhiming Zhou, Zhen Liu *, Yi Pan, Jianqiang Yi

Institute of Automation, Chinese Academy of Sciences, Beijing, 100190, China

ARTICLE INFO

Article history:
Received 26 August 2021
Received in revised form 4 June 2022
Accepted 13 September 2022
Available online 15 September 2022
Communicated by Mrinal Kumar

Keywords:
Spinning missile
Tensor product model transformation
Parallel distributed compensation
Model filtering
Stability analysis

ABSTRACT

In this paper, the controller design and stability analysis for the parameters time-varying model of spinning missiles are investigated. A mathematical model for the spinning missile considering the flight parameters varying with time is proposed. Based on tensor product (TP) model transformation for the spinning missile, the parallel distributed compensation (PDC) state feedback controller is designed, and the stability of the controlled system is analyzed with the tool of linear matrix inequalities (LMIs). Numerical simulations with time-varying parameters are conducted to demonstrate the effectiveness of the proposed controller. The given controller can not only guarantee the steady performance but also the decoupling performance between pitch and yaw channels when used in the flight parameters time-varying spinning missiles.

1. Introduction

Spinning is a technique widely used in axisymmetric tactical missiles and guided missiles for the advantages in interference suppression, such as thrust misalignment, mass eccentricity, aerodynamic asymmetry [1–4]. As is known to all, due to Magnus effect and gyroscopic effect, spinning missiles have coupling in pitch and yaw channels, which is different from non-spinning missiles. In addition, due to the control coupling caused by actuators, the guidance and control systems of spinning missiles are more complex than non-spinning missiles. Thus, control decoupling is necessary to achieve ideal response performance. Many scholars pay attention to decoupling controller design for spinning missiles [5–8]. Moreover, flight parameters such as flight height, speed and spinning rate are time-varying during flight phase. Therefore, overcoming the coupling effect, meanwhile, realizing precise control within the whole flight envelope is a very challenging task.

Before designing spinning missile controller, stability of the system is analyzed commonly. There are many valuable literature reported in investigating the stability of spinning missiles with different control topologies in the last decades, and the related techniques mostly focus on complex summation method and state space method. Using complex summation method, the stability of spinning missiles controlled by different autopilot, e.g., rate loop, attitude autopilot, acceleration autopilot, or guided by homing proportional guidance law was studied in Refs. [9–15]. Also, complex summation method is valid in missiles equipped with various seekers [16–19]. Koohmaskan investigated the stability of spinning missiles induced by hinge moment by expressing the spinning missile system in state space representation, and then checked the eigenvalues of the system to validate the asymptotic stability via an LMIs tool in Ref. [20]. The two aforementioned methods are useful in dealing with linear time invariant (LTI) systems, and the essence of the stability of LTI systems is equivalent to the system matrix eigenvalues symbol judgment. However, there will be great difficulties in deducing the stability condition of spinning missiles within the whole flight envelope, since the spinning missiles are parameter time-varying systems.

As for spinning missiles controller design, there are two main control techniques commonly used. One is based on classic autopilot structure, adopting frequency domain design method, such as pole assignment. And static decoupling approach such as presetting angle is used to guarantee the steady state response of the system [7,11,21–23]. Another is modern robust multi-variable control such as H_2 or H_∞ coupling with interpolation method [24–27] or gain-scheduling control [28–30]. The interpolation method is linearly interpolating the scheduling vector through a number of pre-calculated controller parameters tables. It is simple and easy for engineering implementation. However, it is hard to guarantee the system performance within the whole flight envelope. Moreover, the aforementioned method even cannot guarantee the stability for parameters time-varying systems. The gain-scheduling

* Corresponding author.
E-mail addresses: zhiming.zhou@ia.ac.cn (Z. Zhou), liuzhen@ia.ac.cn (Z. Liu), yi.pan@ia.ac.cn (Y. Pan), jianqiang.yi@ia.ac.cn (J. Yi).

https://doi.org/10.1016/j.ast.2022.107877
1270-9638/

Nomenclature

a_y, a_z	acceleration of missile ..... m/s^2	C_d	drag force coefficient
m	mass of missile ..... kg	C_L	lift force coefficient
V	flight velocity ..... m/s	C'_L	derivative of lift force coefficient
h	flight height ..... m	C_μ	Magnus force coefficient
ρ	atmospheric density ..... kg/m^3	C''_μ	derivative of Magnus force coefficient
q	$\frac{1}{2}\rho V^2$ ..... dynamic pressure	I_x	longitudinal inertial moment ..... kg $\cdot$ s^2
S	reference area ..... m^2	I_t	lateral inertial moment ..... kg $\cdot$ s^2
L	reference length ..... m	m'_x	roll-induced moment coefficient
d	reference diameter ..... m	$m'_{x\omega}$	roll damping moment coefficient
T	thrust force ..... N	$m'_{\sigma x}$	roll control moment coefficient
α^*	full angle of attack ..... rad	m_s	static moment coefficient
α	non-spinning angle of attack ..... rad	m'_s	derivative of static moment coefficient
β	non-spinning sideslip angle ..... rad	m'_σ	control moment coefficient
θ, φ, γ	pitch, yaw, roll angle ..... rad	m'_ω	damping moment coefficient
α_t	canted angle of tails ..... rad	m_μ	coefficient of Magnus moment
σ_y, σ_z	non-spinning actuators angle ..... rad	m''_μ	derivative of coefficient of Magnus moment
σ_{cy}, σ_{cz}	command of non-spinning actuators angle ..... rad	ω_x, ω_y, ω_z	angular rate of frame ..... rad/s

control has many elegant applications on missile control, but the challenging work is how to reduce the conservatism in model establishment, and the numbers of LMIs to be solved increase the difficulty of applications.

There are many works on the stability analysis and controller design based on LTI model about spinning missiles. However, the work on spinning missiles flight control system design involved with coupling effect and linear parameter-varying (LPV) systems model is rarely reported. Addressing the aforementioned issues, this paper adopts the TP model transformation proposed by Baranyi through a series of papers [31–35] to establish the connect between LTI and LPV models of spinning missiles. Then drawing lessons from Takagi-Sugeno (T-S) fuzzy controller design, the controller constrained with decay rate is investigated, and stability of the system is analyzed. Finally, the tracking and decoupling controller is given in the TP form.

The remainder of this paper is organized as follows. In section 2, the LPV model of spinning missiles is given under some assumptions, and the actuator response is modeled by a second order system. In section 3, the principles and procedures of TP model transformation for the spinning missiles are presented. In section 4, the tracking and decoupling controller is designed, and stability of the controlled system is analyzed. In section 5, the simulation results compared with structured H_∞ synthesis are given. Finally, the conclusions are given in section 6.

2. Model of spinning missile

Before establishing the model of spinning missile, some common assumptions are adopted.

A1. The gravity effect is generally excluded for it can be compensated in the autopilots;
A2. The variables α^*, α, β, φ, ψ, $\dot\psi$, $\dot\vartheta$ are small.

Under the small angle assumption, α^*, α, β, φ, ψ are approximately zero, $\dot\psi$, $\dot\vartheta$ are small enough compared to the roll rate $\dot\gamma$, and the coefficients of the aerodynamic moments are linearized, namely, $C_L \approx C'_L\alpha^*$, $C_\mu \approx C''_\mu(\dot\gamma d/V)\alpha^*$, $m_s = m'_s\alpha^*$, $m_\mu \approx m''_\mu(\dot\gamma d/V)\alpha^*$. According to reference [11,15], six degrees-of-freedom dynamic equations of the spinning missiles can be written in the non-spinning frame as:

$$\begin{cases} \dot V = (-qSC_d + T)/m \\ \dot\theta = \frac{qSC'_L+T}{mV}\alpha - \frac{qS}{mV}C''_\mu(\dot\gamma d/V)\beta \\ \dot\varphi = \frac{qSC'_L+T}{mV}\beta - \frac{qS}{mV}C''_\mu(\dot\gamma d/V)\alpha \\ \ddot\gamma = \left(qSLm'_x\alpha_t - qSLm'_{x\omega}(d/V)\omega_x + qSLm'_{\sigma x}\sigma_x\right)/I_x \\ \ddot\vartheta - (I_x/I_t)\dot\gamma\dot\psi = (qSL/I_t)m'_s\alpha - (qSL/I_t)m''_\mu(\dot\gamma d/V)\beta \\ \qquad - (qSL/I_t)m'_\omega(L/V)\dot\psi + (qSL/I_t)m'_\sigma\sigma_z \\ \ddot\psi + (I_x/I_t)\dot\gamma\dot\vartheta = (qSL/I_t)m'_s\beta + (qSL/I_t)m''_\mu(\dot\gamma d/V)\alpha \\ \qquad - (qSL/I_t)m'_\omega(L/V)\dot\vartheta + (qSL/I_t)m'_\sigma\sigma_y \end{cases} \tag{1}$$

From observation in Eq. (1), the terms V and $\dot\gamma$ are independent with other four state variables. Along with the change of V and $\dot\gamma$, by defining $a_1 = \frac{qSC'_L+T}{mV}$, $a_2 = -\frac{qS}{mV}C''_\mu(\dot\gamma d/V)$, $b_{11} = (qSL/I_t)m'_s$, $b_{12} = (qSL/I_t)m''_\mu(\dot\gamma d/V)$, $b_{21} = (I_x/I_t)\dot\gamma$, $b_{22} = (qSL/I_t)m'_\omega(L/V)$, and $c_\sigma = (qSL/I_t)m'_\sigma$, and using the equations that $\theta = \vartheta - \alpha$ and $\varphi = \psi - \beta$, Eq. (1) can be reformulated as

$$\begin{cases} \dot\alpha = \dot\vartheta - a_1\alpha - a_2\beta \\ \dot\beta = \dot\psi - a_1\beta + a_2\alpha \\ \ddot\vartheta = b_{11}\alpha + b_{12}\beta + b_{21}\dot\psi + b_{22}\dot\vartheta + c_\sigma\sigma_z \\ \ddot\psi = b_{11}\beta - b_{12}\alpha - b_{21}\dot\vartheta + b_{22}\dot\psi + c_\sigma\sigma_y \end{cases} \tag{2}$$

Here V is determined by drag force and thrust, $\dot\gamma$ is determined by canted angle of tails and rolling damping moment, which are independent with other state variables. Thus, Eq. (2) can be treated as an LPV system, and the scheduling parameters are the flight velocity and rolling rate. Moreover, the defined symbols such as a_1, b_{11} are linear with the dynamic pressure q, which is a function about flight height. Therefore, the third scheduling parameter is flight height.

The measurement outputs are lateral accelerations expressed as

$$\begin{cases} a_y = V(\vartheta - \alpha) = V(a_1\alpha + a_2\beta) \\ a_z = -V(\psi - \beta) = -V(a_1\beta - a_2\alpha) \end{cases} \tag{3}$$

And the actuators response is modeled by a second order system with natural frequency $1/T_s$ and damping ratio μ_s. The response of the actuators expressed in non-spinning frame can be borrowed from [9] as

$$\begin{bmatrix} \sigma_z \\ \sigma_y \end{bmatrix} = k_s k_r \begin{bmatrix} \cos\gamma_d & \sin\gamma_d \\ -\sin\gamma_d & \cos\gamma_d \end{bmatrix} \begin{bmatrix} \sigma_{cz} \\ \sigma_{cy} \end{bmatrix} \tag{4}$$

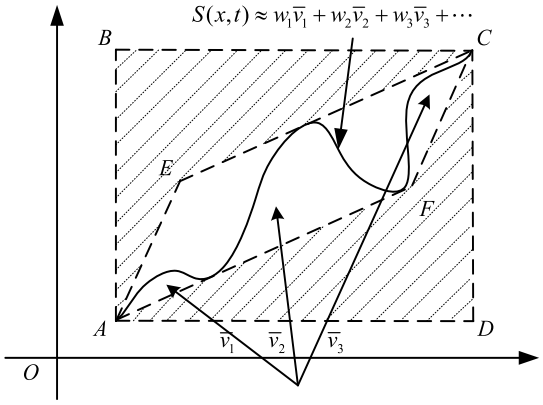

Fig. 1. Polytope LPV system conservatism with vertex selection.

where k_s is the gain of the actuators, $k_r = \frac{1}{\sqrt{(1-T_s^2\dot{\gamma}^2)^2+(2\mu_s T_s\dot{\gamma})^2}}$ is the dynamic gain of the actuators caused by spinning, $\gamma_d = \arccos\frac{1-T_s^2\dot{\gamma}^2}{\sqrt{(1-T_s^2\dot{\gamma}^2)^2+(2\mu_s T_s\dot{\gamma})^2}} + \tau\dot{\gamma}$ is steady-state deviation angle caused by the delay of the actuators dynamics.

Traditional method for the autopilot design is based on characteristic point. However, decoupling controller of spinning missiles designed for the characteristic point can only guarantee good dynamic and decoupling performance at that point, since the flight velocity, height and rolling rate change along with flight trajectory. The method based on the characteristic point cannot guarantee good performance in the whole trajectory. Therefore, gain scheduling is needed. Traditional robust multi-variable control techniques coupling with gain scheduling are conservative in the process of model establishment. As shown in Fig. 1, the parameters time-varying system $S(x,t)$ is generally represented by the polytope LPV system whose vertex systems are composed with A, B, C, D in the missile model, however, it can be represented by the polytope LPV system A, E, C, F with less conservatism. In the next section, the TP model transformation is used to find minimal numbers of vertex systems such as $\bar{v}_1$, $\bar{v}_2$ and $\bar{v}_3$ to approximate the parameters time-varying system $S(x,t)$ with convex combination, which will greatly reduce conservatism in the model establishing.

3. TP model transformation

Consider the following system:

$$\begin{cases} \dot{x}(t) = \mathbf{A}(p(t))x(t) + \mathbf{B}(p(t))u(t) \\ y(t) = \mathbf{C}(p(t))x(t) + \mathbf{D}(p(t))u(t) \end{cases} \tag{5}$$

where $u(t) \in \mathrm{R}^k$, $y(t) \in \mathrm{R}^l$ and $x(t) \in \mathrm{R}^m$ are the control input, system output and system state vector, $p(t)$ represents the time-varying parameter vector in the N-dimensional bounded space $\Theta = [\, a_1 \;\; b_1 \,] \times [\, a_2 \;\; b_2 \,] \times \cdots \times [\, a_N \;\; b_N \,] \in \mathrm{R}^N$. The system matrix is

$$S(p(t)) = \begin{bmatrix} \mathbf{A}(p(t)) & \mathbf{B}(p(t)) \\ \mathbf{C}(p(t)) & \mathbf{D}(p(t)) \end{bmatrix} \in \mathrm{R}^{(m+k)(m+l)} \tag{6}$$

which can be stored as a system tensor. The TP model transformation aims to approximate system (5) with some LTI systems by high-order singular-value decomposition (HOSVD) over the discrete hyperrectangular grid, so that it is possible to use the technique in fuzzy systems or robust gain scheduling.

The core of the TP model transformation is HOSVD. It is known that each matrix can be written as following using the singular value decomposition (SVD) [36]:

$$\mathbf{A} = \mathbf{USV}^T \tag{7}$$

where $\mathbf{A}$ is an $m \times n$ matrix, $\mathbf{U}$ is an $m \times m$ unitary matrix, $\mathbf{V}$ is an $n \times n$ unitary matrix, and $\mathbf{S}$ is an $m \times n$ rectangular diagonal matrix with non-negative real numbers on the diagonal, which is so called singular values. Due to the character of SVD, it is efficient in matrix approximation by dropping some little singular values. In real systems, the system matrices are often shown as high order matrices, or recorded as high order tensors, since the time-varying parameter vector $p(t)$ not only has one dimension. To approximate a high order tensor, SVD should be expanded to HOSVD. The first step is unfolding the system tensor into bidimensional space along one dimension to get a 2-dimensional matrix expression, then applying the SVD on the obtained 2-dimensional matrix. The next step is packing the result back into the tensor form. Finally, repeat the above steps along every dimension resulting in an HOSVD. For a tensor $\mathscr{A}$, the result of HOSVD can be written as

$$\mathscr{A} = \mathscr{S} \times_1 U_{(1)}^T \times_2 U_{(2)}^T \times_3 \cdots \times_N U_{(N)}^T = \mathscr{S} \overset{N}{\underset{n=1}{\otimes}} U_{(n)}^T \tag{8}$$

where $\mathscr{S}$ is the core tensor of $\mathscr{A}$ constructed from the vertex system matrices $S_1, S_2, \cdots, S_N$, $U_{(n)}$ are unitary matrices, $\times_{(n)}$ symbol means n-mode product of a tensor.

Applying HOSVD on the system matrix (6), system (5) can be expressed as

$$\begin{pmatrix} \dot{x}(t) \\ y(t) \end{pmatrix} \approx \left(\mathscr{S} \overset{N}{\underset{r=1}{\otimes}} \omega_r p(t) \right) \begin{pmatrix} x(t) \\ u(t) \end{pmatrix} \tag{9}$$

where $\mathscr{S}$ is the core tensor of system (5), ω_n is coefficient of the corresponding vertex systems. The above formula represents the approximation of the original system, and its error with the original system is as follows

$$\varepsilon = \left\| S(p(t)) - \mathscr{S} \overset{N}{\underset{r=1}{\otimes}} \omega_r p(t) \right\| \leq \sum_k \sigma_k^2 \tag{10}$$

where σ_k is small singular value dropped in the process of HOSVD. For more details about the singular value calculation process one can refer to Ref. [31].

Similar to SVD, the coefficient matrices $U_{(n)}$ are unitary matrices, which do not satisfy the sum normalization (SN) and nonnegative normalization (NN) conditions, thus the results of HOSVD cannot guarantee convexity of the vertex systems. Moreover, polytopic systems have advantages in using LMIs, whose vertex systems satisfy the SN and NN conditions. Therefore, to take advantage of LMIs in controller design for the TP model, it is necessary to normalize the result of HOSVD, which results in

$$\left\{ \forall p(t) : \sum\nolimits_{r=1}^{N} \omega_r(p(t)) = 1, \forall r, p(t) : \omega_r(p(t)) \geq 0 \right\} \tag{11}$$

After that, system (5) can be expressed as

$$\begin{cases} \dot{x}(t) \approx \sum\limits_{r=1}^{N} \omega_r(p(t))(\mathbf{A}_r x(t) + \mathbf{B}_r u(t)) \\ y(t) \approx \sum\limits_{r=1}^{N} \omega_r(p(t))(\mathbf{C}_r x(t) + \mathbf{D}_r u(t)) \end{cases} \tag{12}$$

For further details about the TP model transformation and process of vertex system normalization, one can refer to Ref. [31,35]. According to the above analysis, the TP model transformation can be divided into the following steps:

- Define the scheduling space Θ of the time-varying vector $p(t)$, where $p(t) \in [\, a_1 \;\; b_1 \,] \times [\, a_2 \;\; b_2 \,] \times \cdots \times [\, a_N \;\; b_N \,]$ holds;
- Divide the scheduling space Θ arbitrarily, where the method of average partition can be used;

- Calculate the discrete system matrices in the divided scheduling space and record in the form of high-order tensors;
- Apply HOSVD on the obtained high-order tensor, drop zero or small singular values according to the tolerable error of the model, which will result in a core tensor;
- Normalize the result of HOSVD, make the weight coefficients meet the SN and NN conditions so that the convex combination of the vertex systems can approximate the original system.

There are three advantages in the TP model transformation: firstly, it greatly reduces the numbers of vertex systems, which is conducive to solution of the controller; secondly, it highly restores the original system matrices through the core tensor and weight coefficients, and the error between the original system and the TP model is given quantitatively; thirdly, it avoids the randomness of vertex system selection and reduces the conservatism of controller solution.

4. Controller design and stability analysis

Observing the process of the TP model transformation, the vertex systems can approximate the original system through the convex combination of the weight coefficients, and each vertex system is an LTI system. Thus, the equilibrium of the TP model (12) is globally asymptotically stable if there exists a common positive definite matrix $\mathbf{P}$ such that [37]

$$\mathbf{A}_r^T\mathbf{P} + \mathbf{P}\mathbf{A}_r < 0 \quad r = 1, 2, \cdots, N \tag{13}$$

Therefore, finding a common Lyapunov function for each vertex system satisfy the Lyapunov stability condition can ensure the stability of the original system. Notice that the continuous T-S fuzzy system is expressed as

$$\begin{aligned} &\text{IF } p_1(t) \text{ is } M_{i1} \ \cdots \text{ and } p_n(t) \text{ is } M_{in} \\ &\text{THEN} \begin{cases} \dot{x}(t) = \mathbf{A}_i x(t) + \mathbf{B}_i u(t) \\ y(t) = \mathbf{C}_i x(t) \end{cases} \end{aligned} \tag{14}$$

where the premise variables $p_1(t), \ldots, p_n(t)$ are same as the time-varying parameter vector $p(t)$ in the TP model transformation, the membership degree of the fuzzy set M_{ij} is similar to the coefficients of the vertex systems of the TP model, and the system matrices $\mathbf{A}_i, \mathbf{B}_i, \mathbf{C}_i$ form the vertex systems. Thus the TP model is highly similar to the T-S model except the system matrix $\mathbf{D}_i$. Here the PDC state feedback controller commonly used in T-S fuzzy systems is considered in the follow:

$$\mathbf{K}_r = PDC(S_r), \quad r = 1, 2, \cdots, N \tag{15}$$

Assuming that the PDC controller has the same weight coefficients as the TP model, the control input can be expressed as

$$u(t) = -\left(\sum_{r=1}^{N} \omega_r(p(t))\mathbf{K}_r\right) x(t) \tag{16}$$

In model (12), $\mathbf{D}_r$ is not equal to zero, which will bring extra difficulties in state feedback controller design and stability analysis. Thus, model filtering is implemented. There are two methods, one is pre-filtering the origin control input u, that is

$$\begin{cases} \dot{x}_u = \mathbf{A}_u x_u + \mathbf{B}_u \tilde{u} \\ u = \mathbf{C}_u x_u \end{cases} \tag{17}$$

where $\tilde{u}$ is the new control input. The other method is post-filtering the measurement output y, that is

$$\begin{cases} \dot{x}_y = \mathbf{A}_y x_y + \mathbf{B}_y y \\ \tilde{y} = \mathbf{C}_y y \end{cases} \tag{18}$$

where $\tilde{y}$ is the new control measured output. Here the two methods are implemented meanwhile. Substituting Eq. (17) and (18) into system (5) leads that

$$\begin{aligned} &\begin{bmatrix} \dot{x} \\ \dot{x}_u \\ \dot{x}_y \end{bmatrix} = \begin{bmatrix} \mathbf{A}(p(t)) & \mathbf{B}(p(t))\mathbf{C}_u & 0 \\ 0 & \mathbf{A}_u & 0 \\ \mathbf{B}_y\mathbf{C}(p(t)) & \mathbf{B}_y\mathbf{D}(p(t))\mathbf{C}_u & \mathbf{A}_y \end{bmatrix} \begin{bmatrix} x \\ x_u \\ x_y \end{bmatrix} + \begin{bmatrix} 0 \\ \mathbf{B}_u \\ 0 \end{bmatrix} \tilde{u} \\ &\tilde{y} = \begin{bmatrix} 0 & 0 & \mathbf{C}_y \end{bmatrix} \begin{bmatrix} x \\ x_u \\ x_y \end{bmatrix} \end{aligned} \tag{19}$$

After the process of filtering, the matrix $\mathbf{D}$ of the new model equals to zero. Therefore, without losing generality, here $\mathbf{D}_r = 0$ can be assumed. Substituting the controller into the TP model (12), it obtains that

$$\dot{x}(t) = \sum_{r=1}^{N}\sum_{s=1}^{N} \omega_r(p(t))\omega_s(p(t))(\mathbf{A}_r - \mathbf{B}_r\mathbf{K}_s)x(t) \tag{20}$$

It is equivalent to

$$\begin{aligned} \dot{x}(t) = &\sum_{r=1}^{N} \omega_r(p(t))\omega_r(p(t))\mathbf{G}_{r,r}x(t) \\ &+ 2\sum_{r=1}^{N}\sum_{r<s} \omega_r(p(t))\omega_s(p(t))\frac{\mathbf{G}_{r,s} + \mathbf{G}_{s,r}}{2}x(t) \end{aligned} \tag{21}$$

where $\mathbf{G}_{r,s} = \mathbf{A}_r - \mathbf{B}_r\mathbf{K}_s$ holds. The above system is regarded as the sum of two subsystems. Defining the Lyapunov function of the system as $\mathbf{V}(x(t)) = x(t)^T\mathbf{P}x(t)$, according to Lyapunov stability, if there is a common positive definite matrix $\mathbf{P}$ satisfying

$$\mathbf{G}_{r,r}^T\mathbf{P} + \mathbf{P}\mathbf{G}_{r,r} < 0 \quad r = 1, 2, \cdots, N \tag{22}$$

$$\left(\frac{\mathbf{G}_{r,s} + \mathbf{G}_{s,r}}{2}\right)^T\mathbf{P} + \mathbf{P}\left(\frac{\mathbf{G}_{r,s} + \mathbf{G}_{s,r}}{2}\right) \le 0 \quad r < s \le N, \omega_r \times \omega_s \neq 0 \tag{23}$$

then the PDC controller ensures the quadratic stability of system (12). The above matrix inequalities do not represent LMIs conditions for there is a product of $\mathbf{K}_s$ and $\mathbf{P}$ existing in the inequalities. Multiplying by $\mathbf{P}^{-1}$ on the left and right side of the inequalities, defining $\mathbf{X} = \mathbf{P}^{-1}$ and $\mathbf{M}_r = \mathbf{K}_r\mathbf{X}$, the above matrix inequalities yield Theorem 1.

Theorem 1. *The sufficient condition for the controller (16) to make the system (12) quadratic stable is that there are a positive definite symmetric matrix* $\mathbf{X}$ *and* $\mathbf{M}_r (r = 1, 2 \cdots, N)$ *satisfying*

$$-\mathbf{X}\mathbf{A}_r^T - \mathbf{A}_r\mathbf{X} + \mathbf{M}_r^T\mathbf{B}_r^T + \mathbf{B}_r\mathbf{M}_r > 0, \quad r = 1, 2 \cdots, N \tag{24}$$

$$\begin{aligned} &-\mathbf{X}\mathbf{A}_r^T - \mathbf{A}_r\mathbf{X} - \mathbf{X}\mathbf{A}_s^T - \mathbf{A}_s\mathbf{X} + \mathbf{M}_s^T\mathbf{B}_r^T \\ &+\mathbf{B}_r\mathbf{M}_s + \mathbf{M}_r^T\mathbf{B}_s^T + \mathbf{B}_s\mathbf{M}_r \ge 0, \quad r < s \le N, \omega_r \times \omega_s \neq 0 \end{aligned} \tag{25}$$

If there is a feasible solution to the above LMIs, then the feedback gains can be obtained as

$$\mathbf{K}_r = \mathbf{M}_r\mathbf{X}^{-1} \tag{26}$$

Although Theorem 1 can guarantee the stability of system (12), it cannot guarantee the dynamic performance of the controlled system. Since spinning missiles control system requires fast response, it should add the extra constraint that

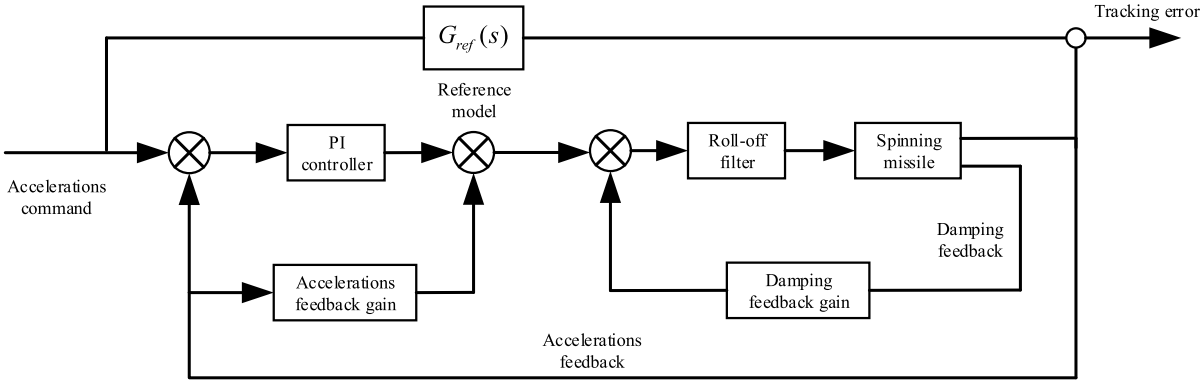

Fig. 2. The diagram of the structured H_∞ synthesis for spinning missile.

$$\dot{\mathbf{V}}(x(t)) \le -2\alpha \mathbf{V}(x(t)) \tag{27}$$

where $\alpha > 0$ determines decay rate of the system. Therefore, α is called decay rate factor. The condition (27) for the controlled system is equivalent to

$$\mathbf{G}_{r,r}^T \mathbf{P} + \mathbf{P}\mathbf{G}_{r,r} + 2\alpha \mathbf{P} < 0 \quad r = 1, 2, \cdots, N \tag{28}$$

$$\left(\frac{\mathbf{G}_{r,s} + \mathbf{G}_{s,r}}{2}\right)^T \mathbf{P} + \mathbf{P}\left(\frac{\mathbf{G}_{r,s} + \mathbf{G}_{s,r}}{2}\right) + 2\alpha \mathbf{P} \le 0$$
$$r < s \le N, \omega_r \times \omega_s \ne 0 \tag{29}$$

Similar to the derivation of Theorem 1, it obtains the following theorem.

Theorem 2. *The sufficient condition for the controller (16) to make the system (12) quadratic stable with a decay rate α is that there are a positive definite symmetric matrix $\mathbf{X}$ and $\mathbf{M}_r (r = 1, 2 \cdots, N)$ satisfying*

$$-\mathbf{X}\mathbf{A}_r^T - \mathbf{A}_r\mathbf{X} + \mathbf{M}_r^T\mathbf{B}_r^T + \mathbf{B}_r\mathbf{M}_r - 2\alpha\mathbf{X} > 0, \quad r = 1, 2 \cdots, N \tag{30}$$

$$-\mathbf{X}\mathbf{A}_r^T - \mathbf{A}_r\mathbf{X} - \mathbf{X}\mathbf{A}_s^T - \mathbf{A}_s\mathbf{X} + \mathbf{M}_s^T\mathbf{B}_r^T + \mathbf{B}_r\mathbf{M}_s + \mathbf{M}_r^T\mathbf{B}_s^T + \mathbf{B}_s\mathbf{M}_r - 4\alpha\mathbf{X} \ge 0, \quad r < s \le N, \omega_r \times \omega_s \ne 0 \tag{31}$$

If there is a feasible solution to the above LMIs, then the feedback gains can be obtained as

$$\mathbf{K}_r = \mathbf{M}_r\mathbf{X}^{-1} \tag{32}$$

Although Theorem 2 can stabilize the spinning missiles system, special considerations must be given to the tracking of reference commands and the decoupling of the spinning missiles system. Assume that the reference input is $v(t)$, the feedforward gain matrices of the vertex systems are denoted as $\mathbf{L}_r$. There are many ways to design the gain matrices $\mathbf{L}_r$, but all of them should guarantee the steady-state gain of the system. For spinning missiles, the general reference input is lateral acceleration, that means the steady gain of the system is $\tilde{\mathbf{D}} = diag(d_{11}, d_{22})$, where the diagonal matrix decouples yaw and pitch channels, and $d_{11} = d_{22} = 1$ guarantees the gain of the system when the system reaches the steady response. Referring to the commonly used static decoupling algorithm, the gain adjustment matrix at each vertex system can be calculated as

$$\mathbf{L}_r = -\left[\mathbf{C}_r(\mathbf{A}_r - \mathbf{B}_r\mathbf{K}_r)^{-1}\mathbf{B}_r\right]^{-1}\tilde{\mathbf{D}} \quad r = 1, 2, \cdots, N \tag{33}$$

The feedforward gain matrices $\mathbf{L}_1, \cdots, \mathbf{L}_N$ form high order tensor $\mathscr{L}$, and controller gain matrices form high order tensor $\mathscr{K}$. Then the control can be given in the TP form as

Table 1
Spinning missile's flight parameters.

Parameter	Value	Parameter	Value
C_L'	10.3	m_μ''	−0.168
m_s'	−0.6589	C_μ''	−0.0087
m_ω'	1.777	m_σ'	0.0546
I_x	5.23	I_t	1.65e3
$\dot{\gamma}$	6π	m	465
L	6.54	d, m	0.15
k_s	1.0	τ	0.005
μ_s	0.5	T_s	0.008

$$u(t) = \left(\mathscr{K} \overset{N}{\underset{n=1}{\otimes}} \omega_n p(t)\right) x(t) + \left(\mathscr{L} \overset{N}{\underset{n=1}{\otimes}} \omega_n p(t)\right) v(t) \tag{34}$$

5. Simulation results

According to the analysis of the scheduling variables of spinning missiles, it shows that the flight velocity, rolling rate and flight height are the key factors affecting the dynamic performance of spinning missiles. While the mass and thrust of spinning missiles generally remain unchanged in the controlled phase, and the rolling rate does not change much. Therefore, the scheduling variables selected in this section are flight velocity and height. Table 1 lists the spinning missile's flight parameters.

Because Magnus forces have very little influence comparing with other dynamic terms, a_2 will be ignored in this section for the controller design convenience, that means $a_2 \equiv 0$. The atmospheric density is fitted by polynomial as $\rho = 1.219 - 1.123 \times 10^{-4}h + 3.448 \times 10^{-9}h^2 - 3.33010^{-14}h^3$. In this section, the spinning missile flight velocity varies in $[600, 1000]$ m/s, and flight height varies in $[0, 10000]$ m. Before implementing the PDC controller, as a contrast, here structured H_∞ synthesis is adopted to control and decouple the spinning missile. Refer to Ref. [38], the diagram of the structured H_∞ synthesis for the spinning missiles is shown in Fig. 2. The reference model is selected as

$$G_{ref}(s) = \begin{bmatrix} \dfrac{\omega_n^2}{s^2 + 2\xi\omega_n s + \omega_n^2} & 0 \\ 0 & \dfrac{\omega_n^2}{s^2 + 2\xi\omega_n s + \omega_n^2} \end{bmatrix} \tag{35}$$

with $\xi = 0.8$ and $\omega_n = 3$. The diagonal form of G_{ref} guarantees the decoupling performance. To validate the structured H_∞ synthesis, here we select two points $V = 600$ m/s, $h = 10000$ m and $V = 1000$ m/s, $h = 0$ m, and the controlled system step response is shown in Fig. 3 and 4. The results show that the structured H_∞ controller performances well at the character point and decouples the yaw and pitch channels when the controlled system reaches steady-state.

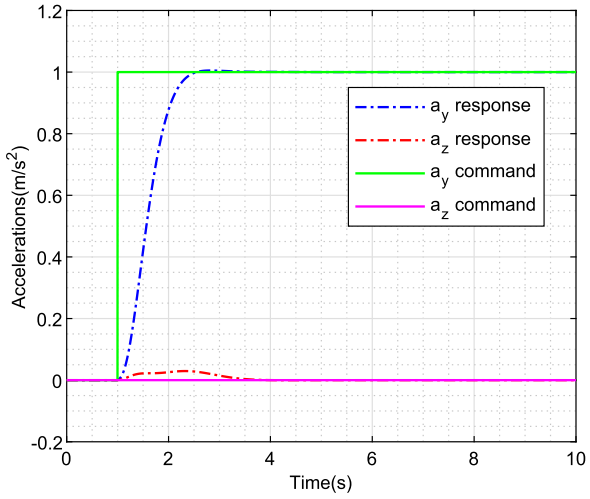

Fig. 3. Step responses of H_∞ synthesis controller at $V = 600$ m/s, $h = 10000$ m.

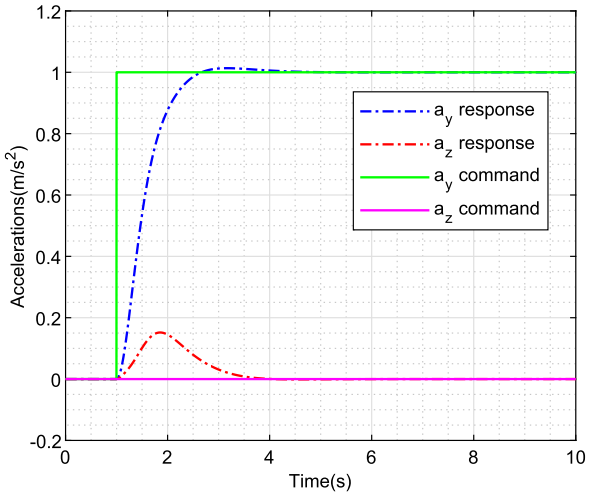

Fig. 4. Step responses of H_∞ synthesis controller at $V = 1000$ m/s, $h = 0$ m.

Here we apply the structured H_∞ controller to the parameters time-varying spinning missile system, where the flight velocity changes from 600 m/s to 1000 m/s, and flight height changes from 10000 m to 0. To realize the spinning missile control along the flight envelope while flight velocity and height vary, here we divide the flight velocity into 10 equal parts, and divide flight height into 10 equal parts. Hence we obtain 100 character points, and calculate the control parameters with interpolating the flight velocity and height. Fig. 5 shows the system step response along the time-varying flight trajectory. Fig. 6 shows the responses of the angle of attack and angle of sideslip.

Fig. 5 shows that, with flight velocity and height changing, the interpolated structured H_∞ controller can realize the command following approximately along flight envelope, but the performances are not as good as the performances on the character points, especially when the flight velocity grows. In addition, it can be seen from Fig. 6 that at the beginning of the simulation, when the flight velocity is low and the flight height is high, the angle of sideslip required to generate the unit lateral acceleration is large. With the increase of the flight velocity and the decrease of the flight height, the dynamic pressure increases, and the angle of sideslip required to generate the unit lateral acceleration gradually decrease.

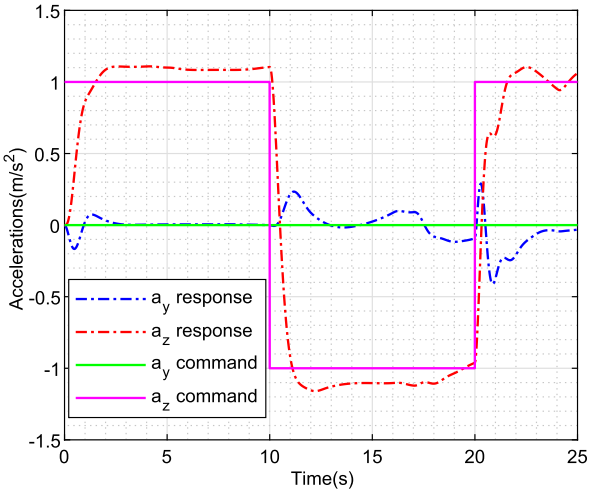

Fig. 5. Step responses of interpolated H_∞ synthesis controller along flight trajectory.

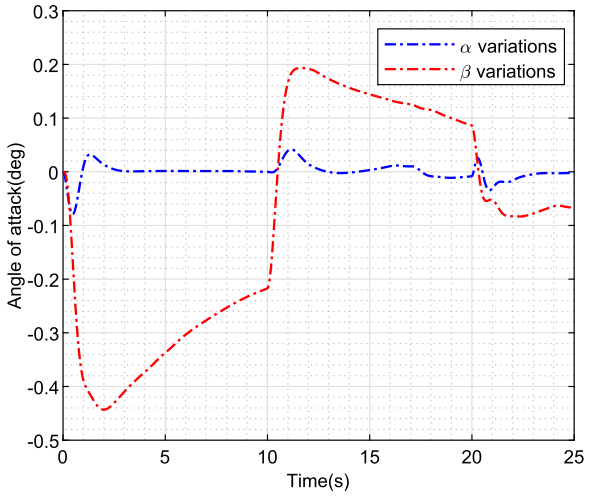

Fig. 6. α, β variations of interpolated H_∞ synthesis controller.

Table 2
Parts of singular values of system tensor.

Modes	3 mode	4 mode
Singular values	55468.1174	55468.0978
	64.1112	79.2811
	3.0150	1.4234e-11
	4.9581e-11	7.3962e-12

In the second part, the TP model transformation and the PDC controller with decay rate factor are employed. In the first step, divide the flight speed into 100 equal parts, and divide flight height into 100 equal parts. Then we obtain the system tensor $\mathscr{S}(V,h)^{6\times6\times100\times100}$ which is formed by the system matrices. Applying HOSVD on the obtained high-order tensor, parts of singular values are list in Table 2. It can be seen that after dropping the small singular value, the vertex systems are only $3 * 2 = 6$, which greatly simplifies the amount of calculation and reduces the difficulty of controller design. The weight coefficients of the vertex systems are shown in the Fig. 7.

Take the character point $V = 600$ m/s, $h = 10000$ m as an example. Here the results of no decay rate constraint and with decay rate $\alpha = 1.5$ are compared in Fig. 8.

It can be seen from Fig. 8 that if there is no decay rate constraint, the controller can make the system stable, but the response

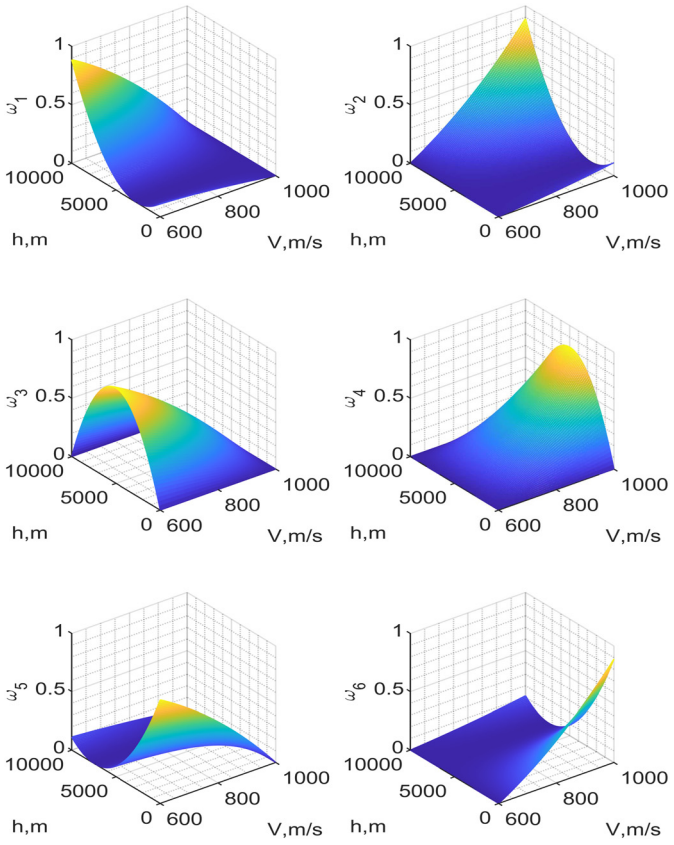

Fig. 7. The weight coefficient of the vertex system.

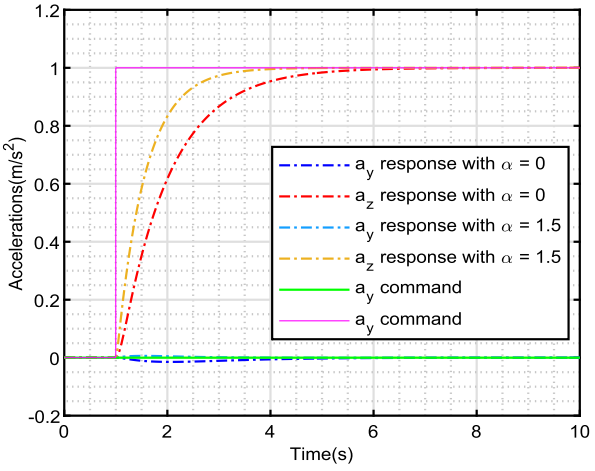

Fig. 8. Step responses of TP controller with/without decay rate at $V = 600$ m/s, $h = 10000$ m.

time is too long, which limits its application in real systems. When the decay rate $\alpha = 1.5$ holds, the system can be stable quickly, which is suitable for practical application.

Applying the TP model transformation and the designed controller to the parameters time-varying spinning missile system, where the simulation conditions are the same with the structured H_∞ synthesis. The following simulation results Fig. 9 and 10 show the performance and decoupling effect of the designed TP controller.

Compared with the results of interpolation in the structured H_∞ synthesis controller, the dynamic decoupling performance of the proposed controller based on the TP model is better, and the decoupling effect between pitch and yaw channels is more obvious.

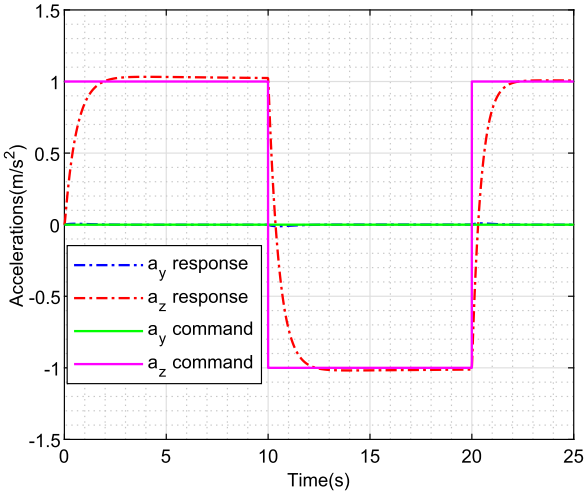

Fig. 9. Step responses of TP controller.

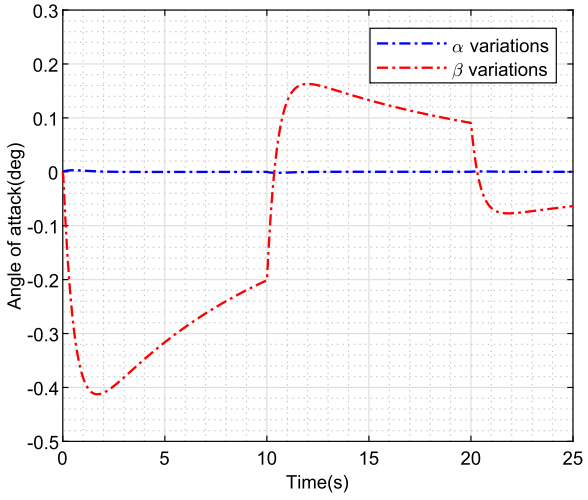

Fig. 10. α, β variations of TP controller.

To enhance the applicability of proposed method, the uncertainties such as wind and control command delay are considered. Consider an external disturbance such as wind with velocity 50 m/s acting on the spinning missile, the designed controller performs as in the Fig. 11. The results reveal that the decoupling performance is guaranteed under the disturbance of wind, however, the steady gain of the controlled system becomes greater for it depends on the measurements of flight velocity. Moreover, the control command delay is tested on the controlled system, and it is found that the designed controller can maintain the performance when the control command delay is no larger than 5 ms. Fig. 12 presents the response of the controlled system under 6 ms control command delay. As the velocity grows up in the terminal phase, the responses are getting unsteady, since the system with high speed is more sensitive to the control command delay.

6. Conclusion

By TP model transformation, the decoupling PDC state feedback controller is designed and the stability of the controlled system is analyzed for the parameters time-varying spinning missiles model. The simulation results compared with H_∞ synthesis controller verify the effectiveness and benefits of the proposed methods. In the design of controllers for parameters time-varying spinning missiles, the work in this paper can be considered for the reason that

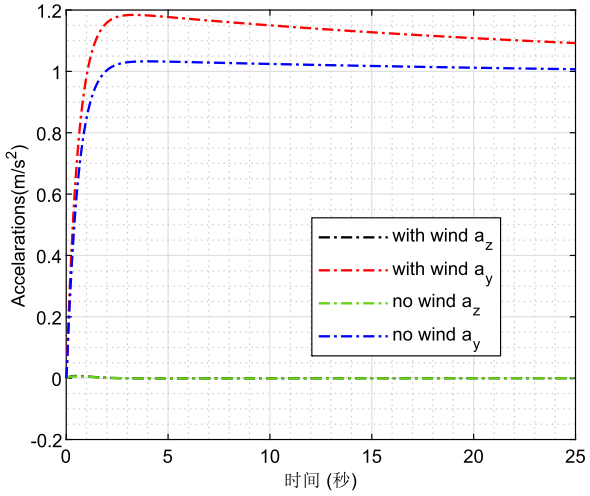

Fig. 11. Step responses with/without wind.

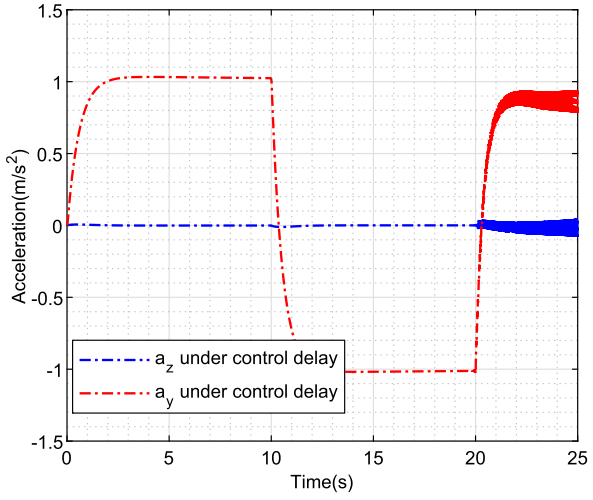

Fig. 12. Step responses under command delay.

the proposed controller can ensure the system stability and dynamic performance under the condition of large-scale parameters time varying. Future work will take the model uncertainties and control command delay into consideration to design globally stable controllers for parameters time-varying spinning missiles.

Declaration of competing interest

The authors declare that they have no known competing financial interests or personal relationships that could have appeared to influence the work reported in this paper.

Acknowledgements

This work was supported by the National Key Research and Development Program of China under Grant 2018AAA0102402, in part by the National Natural Science Foundation of China under Grant 61906197, and in part by the Foundation under Grant 2019-JCJQ-ZD-049.

References

[1] C.H. Murphy, Free flight motion of symmetric missile, Rept. 1216, The Ballistic Research Laboratory, Maryland, 1963.
[2] C.H. Murphy, Effect of roll on dynamic instability of symmetric missiles, J. Guid. Control Dyn. 24 (1957) 673–674.
[3] R.X. Meyer, Coning instability of spacecraft during periods of thrust, J. Spacecr. Rockets 33 (6) (1996) 781–788.
[4] G.R. Cooper, Spinning projectile with an inviscid liquid payload impregnating porous media, AIAA J. 46 (3) (2008) 783–787.
[5] Q. Xu, S. Chang, Z. Wang, Acceleration autopilot design for gliding guided projectiles with less measurement information, Aerosp. Sci. Technol. 77 (2018) 256–264.
[6] M. Abadir, S. Yusuf, A. Pontillo, et al., Parameters estimation methodology for the nonlinear rolling motion of finned cylindrical body, Aerosp. Sci. Technol. 84 (1) (2019) 782–798.
[7] S. Fan, T. Song, J. Wang, et al., Coupling analysis and dynamic stability boundary of spinning missiles considering actuator dynamics and autopilot, Aerosp. Sci. Technol. 111 (2021) 106481, https://doi.org/10.1016/j.ast.2020.106481.
[8] Z. Shi, L. Zhao, Z. Jie, Variational method based robust adaptive control for a guided spinning rocket, Chin. J. Aeronaut. 34 (3) (2021) 164–175.
[9] X. Yan, S. Yang, C. Zhang, Coning motion of spinning missiles induced by the rate loop, J. Guid. Control Dyn. 33 (5) (2010) 1490–1499.
[10] X. Yan, S. Yang, F. Xiong, Stability limits of spinning missiles with attitude autopilot, J. Guid. Control Dyn. 34 (1) (2011) 278–283.
[11] K. Li, S. Yang, L. Zhao, Stability of spinning missiles with an acceleration autopilot, J. Guid. Control Dyn. 35 (3) (2012) 774–786.
[12] K. Li, S. Yang, L. Zhao, Three loop autopilot of spinning missiles, Proc. Inst. Mech. Eng., G J. Aerosp. Eng. 228 (7) (2013) 1195–1201.
[13] W. Zhou, S. Yang, J. Dong, Coning motion instability of spinning missiles induced by hinge moment, Aerosp. Sci. Technol. 30 (2013) 239–245.
[14] G. Liano, J. Castillo, P. Garcia-Ybarra, Steady states of the rolling and yawing motion of unguided missiles, Aerosp. Sci. Technol. 59 (2016) 103–111.
[15] X. Hu, S. Yang, F. Xiong, et al., Stability of spinning missile with homing proportional guidance law, Aerosp. Sci. Technol. 71 (2017) 546–555.
[16] S. He, D. Lin, J. Wang, Coning motion stability of spinning missiles with strapdown seekers, Aeronaut. J. 120 (1232) (2016) 1566–1577.
[17] D. Zheng, D. Lin, J. Wang, et al., Dynamic stability of rolling missiles employing a two-loop autopilot with consideration for the radome aberration parasitic feedback loop, Aerosp. Sci. Technol. 61 (2017) 1–10.
[18] S. Tian, D. Lin, J. Wang, et al., Dynamic stability of rolling missiles with angle-of-attack feedback three-loop autopilot considering parasitic effect, Aerosp. Sci. Technol. 71 (2017) 592–602.
[19] W. Li, Q. Wen, Y. Yang, Stability analysis of spinning missiles induced by seeker disturbance rejection rate parasitical loop, Aerosp. Sci. Technol. 90 (2019) 194–208.
[20] Y. Koohmaskan, M. Arvan, A. Vali, et al., Dynamic stability conditions for a rolling flight vehicle applying continuous actuator, Aerosp. Sci. Technol. 42 (2015) 451–458.
[21] S. Fan, G. Wu, Y. Sun, et al., Analysis of control coupling characteristic and forward decoupling technique for rolling missile, J. Syst. Eng. Electron. 39 (2) (2017) 398–403 (in Chinese).
[22] K. Li, Y. Yu, L. Zhao, Three loop topologies scheme of spinning missiles with decoupling control, in: Automatic Control and Artificial Intelligence International Conference, January 2012.
[23] S. Wang, J. Shan, Three-channel autopilot design for spinning missile, in: 2020 IEEE 5th Information Technology and Mechatronics Engineering Conference, 2020, pp. 952–960.
[24] Z. Guo, X. Yao, X. Zhang, Robust gain scheduled longitudinal autopilot design for rockets during the sustaining phase, Proc. Inst. Mech. Eng., Part I, J. Syst. Control Eng. 230 (10) (2016) 1154–1163.
[25] S. Theodoulis, V. Gassmann, P. Wernert, Guidance and control design for a class of spin-stabilized fin-controlled projectiles, J. Guid. Control Dyn. 36 (2) (2013) 517–531.
[26] S. Theodoulis, F. Seve, P. Wernert, Robust gain-scheduled autopilot design for spin-stabilized projectiles with a course-correction fuze, Aerosp. Sci. Technol. 42 (2015) 477–489.
[27] G. Strub, S. Theodoulis, V. Gassmann, et al., Gain-scheduled autopilot design and validation for an experimental guided projectile prototype, J. Guid. Control Dyn. 42 (2) (2018) 461–475.
[28] P. Apkarian, J. Biannic, Self-scheduled H_∞ control of missile via linear matrix inequalities, J. Guid. Control Dyn. 18 (3) (1995) 532–538.
[29] W. Zhou, Dynamic stability and robust gain-scheduling control of spinning missiles, Doctor thesis, Beijing Institute of Technology, 2016.
[30] B. Lei, P. Shi, C. Chang, et al., Gain-scheduling attitude control for complex spacecraft based on HOSVD, J. Dyn. Syst. Meas. Control 141 (3) (2019) 034503, https://doi.org/10.1115/1.4041752.
[31] P. Baranyi, TP model transformation as a way to LMI-based controller design, IEEE Trans. Ind. Electron. 51 (2) (2004) 387–400.
[32] P. Baranyi, A. Várkonyi-Kóczy, TP transformation based dynamic system modeling for nonlinear control, IEEE Trans. Instrum. Meas. 54 (6) (2005) 2197–2203.
[33] P. Baranyi, Y. Yam, Case study of the TP-model transformation in the control of a complex dynamic model with structural nonlinearity, IEEE Trans. Ind. Electron. 53 (3) (2006) 895–904.
[34] A. Szollosi, P. Baranyi, Influence of the tensor product model representation of q-LPV models on the feasibility of linear matrix inequality based stability analysis, Asian J. Control 20 (3) (2018) 1–17.

[35] P. Baranyi, How to vary the input space of a TS fuzzy model: a TP model transformation based approach, IEEE Trans. Fuzzy Syst. (2020), https://doi.org/10.1109/TFUZZ.2020.3038488.
[36] Z. Petres, P. Baranyi, P. Korondi, et al., Trajectory tracking by TP model transformation: case study of a benchmark problem, IEEE Trans. Ind. Electron. 54 (3) (2007) 1654–1663.
[37] K. Tanaka, M. Sugeno, Stability analysis and design of fuzzy system control systems, Fuzzy Sets Syst. 45 (2) (1992) 135–156.
[38] P. Gahinet, P. Apkarian, Structured H_∞ synthesis in MATLAB, in: Proceedings of the 18th World Congress: The International Federation of Automatic Control, Milano (Italy), August 2011.